

Chemistry of burning the forest floor during the FROSTFIRE experimental burn, interior Alaska, 1999

J. W. Harden,¹ J. C. Neff,^{2,3} D. V. Sandberg,⁴ M. R. Turetsky,¹ R. Ottmar,⁵
G. Gleixner,⁶ T. L. Fries,¹ and K. L. Manies¹

Received 24 November 2003; revised 15 April 2004; accepted 24 June 2004; published 28 August 2004.

[1] Wildfires represent one of the most common disturbances in boreal regions, and have the potential to reduce C, N, and Hg stocks in soils while contributing to atmospheric emissions. Organic soil layers of the forest floor were sampled before and after the FROSTFIRE experimental burn in interior Alaska, and were analyzed for bulk density, major and trace elements, and organic compounds. Concentrations of carbon, nutrients, and several major and trace elements were significantly altered by the burn. Emissions of C, N, and Hg, estimated from chemical mass balance equations using Fe, Al, and Si as stable constituents, indicated that 500 to 900 g C and up to 0 to 4×10^{-4} g Hg/m² were lost from the site. Calculations of nitrogen loss range from -4 to $+6$ g/m² but were highly variable (standard deviation 19), with some samples showing increased N concentrations post-burn potentially from canopy ash. Noncombustible major nutrients such as Ca and K also were inherited from canopy ash. Thermogravimetry indicates a loss of thermally labile C and increase of lignin-like C in char and ash relative to unburned counterparts. Overall, atmospheric impacts of boreal fires include large emissions of C, N and Hg that vary greatly as a function of severe fire weather and its access to deep organic layers rich in C, N, and Hg. In terrestrial systems, burning rearranges the vertical distribution of nutrients in fuels and soils, the proximity of nutrients and permafrost to surface biota, and the chemical composition of soil including its nutrient and organic constituents, all of which impact C cycling. *INDEX TERMS*: 0315 Atmospheric Composition and Structure: Biosphere/atmosphere interactions; 0330 Atmospheric Composition and Structure: Geochemical cycles; 1615 Global Change: Biogeochemical processes (4805); 1030 Geochemistry: Geochemical cycles (0330); *KEYWORDS*: combustion, experimental burn, boreal forest, black spruce, feathermoss, Hg

Citation: Harden, J. W., J. C. Neff, D. V. Sandberg, M. R. Turetsky, R. Ottmar, G. Gleixner, T. L. Fries, and K. L. Manies (2004), Chemistry of burning the forest floor during the FROSTFIRE experimental burn, interior Alaska, 1999, *Global Biogeochem. Cycles*, 18, GB3014, doi:10.1029/2003GB002194.

1. Introduction

[2] Emissions and ash deposition from wildfires have important impacts on atmospheric and watershed chemistry [Liu *et al.*, 2000; Van Wyk *et al.*, 1992], forest biogeochemical cycling [Trabaud, 1994], and the types and rates of vegetative regrowth [Luc and Luc, 1998; Schimel and Granstrom, 1989]. Fires are particularly widespread and severe in boreal forests [Kasischke and Stocks, 2000]

and can lead to major changes in the elemental composition of soils and vegetation. In particular, fires can lead to combustion losses of organic matter and nutrients, changes in the availability of plant nutrients, and mobilization of particulates into the atmosphere, soils, and streams.

[3] One of the most crucial issues involving fire in boreal systems is the impact of burning on carbon cycling, as fire events release CO₂, CH₄, and CO directly to the atmosphere. Reliable post-burn estimates of fire emissions are problematic, however, in part because changes must be reconstructed from control-experiment comparisons and control sites are difficult to identify [see, e.g., Conard and Ivanova, 1998; French *et al.*, 2000]. Changes in budgets and availability of nutrients also impact post-fire regrowth and carbon cycling. In particular, N can be lost through combustion and leaching [Wan *et al.*, 2001]; therefore forests can be limited by nitrogen availability during regrowth [Van Cleve, 1973; Van Cleve and Oliver, 1982].

[4] Burns do not have uniform effects on nutrients, and previous field and laboratory studies [e.g., Dyreness and Norum, 1983] have demonstrated how the heterogeneity of

¹U.S. Geological Survey, Menlo Park, California, USA.

²U.S. Geological Survey, Denver Federal Center, Denver, Colorado, USA.

³Now at Geological Sciences and Environmental Studies, University of Colorado, Boulder, Colorado, USA.

⁴Pacific Northwest Research Station, USDA Forest Service, Corvallis, Oregon, USA.

⁵Seattle Forestry Science Laboratory, Seattle, Washington, USA.

⁶Max Planck Institute for Biogeochemistry, Jena, Germany.

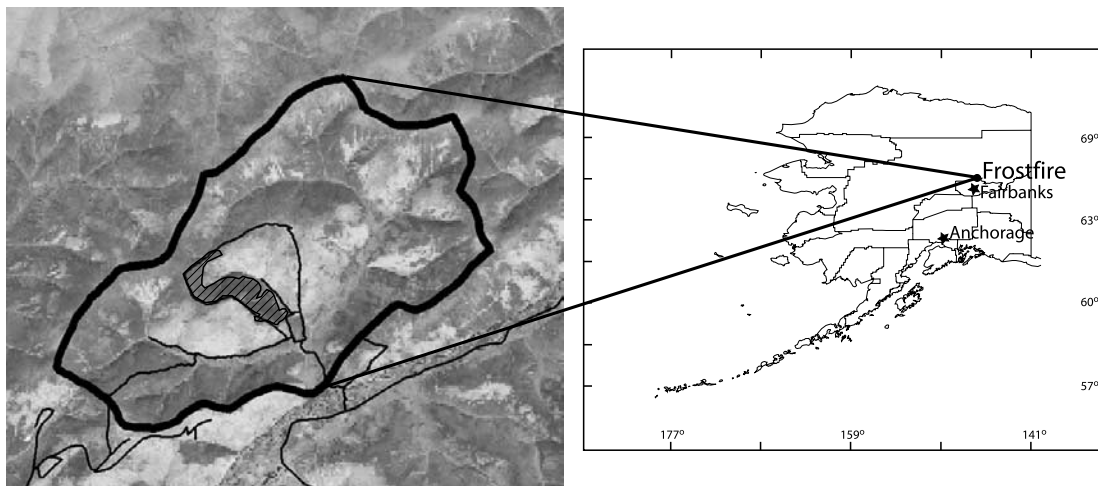


Figure 1. Location of sample sites in interior Alaska.

plant, soil, and moisture content affects fire behavior, post-burn nitrogen availability, and the plant structure and rates of regrowth [Driscoll *et al.*, 1999]. Spatial heterogeneity, post-fire mixing of soil layers, and the difficulty of reconstructing soil horizon structure all add to the complication of estimating fire effects on element concentrations.

[5] Experimental burns offer a unique opportunity to characterize fuels, burn severity, fuel consumption, and the chemical composition of fuel and combustion products. Through measurements before and after fire, the FROSTFIRE experimental burn [see *Hinzman et al.*, 2003] facilitated a direct assessment of fire impacts on element budgets. We focus on characterizing the physical and chemical changes to the forest soils and on assessing the potential for changes in both availability and mobility of multiple elements as the result of fire.

2. Methods

[6] Sampling sites are located within the Caribou Poker Watershed of the University of Alaska's Long-Term Ecological Research (LTER) site, about 60 km north of Fairbanks (Figure 1). All sites described here were placed along transects marked and sampled by the U.S. Forest Service's Fire and Environmental Research Applications Team (FERA). Our sites included the (1) upper black spruce (UPBS) site, located in the closed black spruce canopy near Helmer's Ridge, which burned after torching the base of the slope (Figure 1), and (2) the large black spruce (LBS) site that also burned during the experiment; this site is more poorly drained and is located at the base of the watershed along Poker Creek. Several other sites were characterized but did not burn and are not discussed in this paper.

[7] Before the burn, a number of metal pins (reduction pins) were inserted into the soil where the top of the pin lies flush with the moss surface. Forest floor/organic soil layers were characterized according to forestry nomenclature, which we further interpreted into soil nomenclature [Canadian Agricultural Services Coordinating Committee, 1998; *Soil Survey Staff*, 1998]: (1) live moss (LM) layers are

green and generally contain some leaf and needle litter (Figure 2); (2) dead moss (DM) layers are comprised of undecomposed or slightly decomposed fibric organic horizons that contain a larger portion of moss detritus than roots; (3) upper duff (UD) layers vary in degree of decomposition but are layers in which roots are more abundant than recognizable moss parts; UD layers would in most cases be considered fibric (F) layers (Canadian soil system) or Oi layers (U.S. system); (4) lower duff (LD) layers have some mineral content but are generally well decomposed with no or few recognizable plant parts other than roots. LD layers

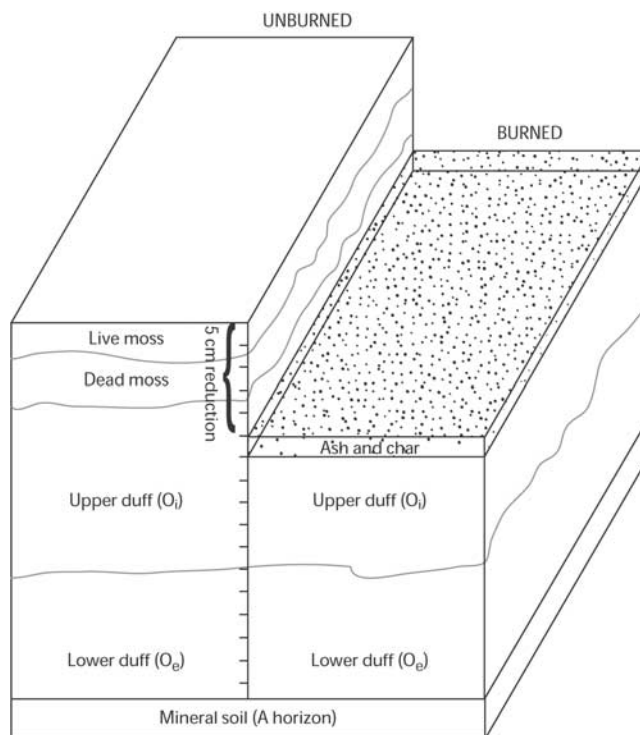


Figure 2. Schematic diagram of soil layers and sampling of ash/char layers after burning.

are mesic or humic (Canadian) horizons or Oe horizons (United States), indicating high degree of decomposition. Before the burn, samples were collected by U.S. Forestry Service personnel and divided into the four soil layers (LM, DM, UD, LD). If thicker than 5 cm, layers were further subdivided.

[8] Bulk density was measured throughout the spring and summer prior to the burn. The most common method for bulk density measurements employed a metal square measuring 20 cm³ with an open top and bottom. This square was driven to the depth of ice or mineral soil to extrude soil. Material then was divided into soil layers or finer-scale depth increments (if thicker than 5 cm). In some instances, bulk density samples were excavated in situ using a three-sided metal box open to a pit face; the depth of each layer was recorded along with the area of the sample box. Samples were weighed within 24 hours, and then were either air dried to a constant mass (mass lost equivalent to air-dry moisture content), or placed into a 65°C oven for 96 hours for oven-dry masses (mass lost equivalent to oven-dry moisture contents).

[9] Within 24 hours of the burn, two sets of samples were collected from the Helmer's Ridge UPBS site, including soil profiles and surface ash-char. For the profile samples, surface ash-char layers were collected volumetrically within a set square to the depth of the lower boundary of black char using a small vacuum. Soil layers (DM, UD, LD) below ash and char layers were collected volumetrically. Each profile was excavated adjacent to a reduction pin (see above) to allow us to relate soil chemical properties to estimates of fire consumption (centimeters of forest soil consumed) (Figure 2). For each soil layer/sample, we noted depth relative to the moss surface. In addition to the profiles, we also collected a series of surface samples adjacent to reduction pins. This set includes only volumetric samples of the ash/uppermost char layer (i.e., excluding deeper unburned material) and depths to mineral soil were recorded.

3. Physical and Chemical Analyses

[10] Material >2 mm and twigs/roots >1 cm diameter were removed, and the samples were ground to pass a 100 mesh screen. Subsamples were analyzed for organic matter content by loss on ignition (LOI) by placing them in platinum crucibles and heating to 550°C for 5 hours and measuring percent mass loss. Hg concentration was measured by a XRAL Inc. digestion with a mixture of H₂SO₄, HNO₃, HCl, and KMnO₄ (5%) and K₂S₂O₈ (5%) in a water bath for 1 hour. Excess KMnO₄ was reduced by hydroxylamine sulfate solution, and Hg (II) was reduced by a SnCl₂ solution. The Hg vapor was separated and measured using a LEEMAN PS200 Automated Mercury Analyzer. Major, minor, and trace elements were measured by inductively coupled plasma-atomic emission spectrometry (ICP-AES). Samples were decomposed using a mixture of HCl, HNO₃, HClO₄, and HF acids at low temperature [Crock *et al.*, 1983]. The digested sample was aspirated into the ICP-AES discharge where the elemental emission signal was measured simulta-

neously for several elements. Calibration was performed by standardizing with digested rock reference materials and a series of multielement solution standards.

[11] Total percent carbon (TC) were made using either a LECO carbon determinator (WR-112) or a Fisons NA1500 elemental analyzer (EA)/Optima isotope ratio mass spectrometer (IRMS). For this analysis, between 1 and 30 mg of sample, depending on the estimated carbon concentration, was loaded into a tin capsule, and the capsule was tightly crimped to exclude atmospheric gases. Samples were then combusted at 1000°C in a stream of oxygen. We also used the Fisons NA1500 EA/Optima IRMS to determine the ¹³C and ¹⁵N abundance. Elemental concentrations were calculated based on instrument responses for calibration standards. In addition to calibration materials, three standard materials were routinely included in all EA/IRMS sample runs. Standards included (1) ethylene diamine tetracetic acid EDTA) obtained from Fisons Instruments, S.p.a., (2) a marine sediment (MESS-1) issued by the Chemistry Division of the Canadian National Research Council, and (3) a river sediment (NBS 1645) issued by the National Bureau of Standards (now the National Institute of Standards and Technology). Precision estimates, expressed as relative standard deviation, were 3.6–6.5% for total carbon and 3.7–6.5% for total nitrogen. Standard deviation for ¹³C for the standard materials was 0.16 to 0.3 per mil (see also *Manies et al.* [2002] for more information on standards). Approximately 3% of all samples were also analyzed in duplicate. For these duplicate runs, standard deviation of duplicate runs averaged <1% for total carbon and <2% for total nitrogen.

[12] Thermogravimetry of the samples was performed with a TGA851e (Mettler-Toledo, Giessen, Germany) according to methods of *Gleixner et al.* [2002]. About 10 mg soil was weighed into 150- μ l aluminum oxide sample cups. The samples were placed at 60°C into the TG analyzer, which was flushed with a constant flow of oxygen. After 25 min the sample was heated at 20°C/min to a final temperature of 1000°C. To reach thermal equilibrium, the temperature was held for 5 min.

[13] The ¹⁴C content of ground, untreated soil was measured by vacuum sealing a homogenized sample containing ~1 mg C with cupric oxide and elemental silver in a quartz tube and combusting at 850°C. The CO₂ produced was purified cryogenically and reduced to graphite using a modified reduction method with titanium hydride, zinc, and cobalt catalyst [Vogel, 1992]. The graphite target is measured directly for ¹⁴C at Lawrence Livermore National Laboratory, Center for Accelerator Mass Spectrometry. The ¹⁴C data are expressed in Delta notation ($\delta^{14}\text{C}$) similar to $\delta^{13}\text{C}$ above, i.e., the deviation in the ¹⁴C/C in parts per thousand (‰) from a standard ($(^{14}\text{C}/\text{C})_{\text{standard}} = 1.176 \times 10^{-12}$), with additional correction for possible fractionation effects based on ¹³C [see *Stuiver and Polach*, 1977]. To convert $\delta^{14}\text{C}$ values to percent Modern (*pM*) values, simply divide by 10 and add 100; $\delta^{14}\text{C} = 0\text{‰}$ (i.e., 100 *pM* or $^{14}\text{C}/\text{C} = 1.176 \times 10^{-12}$) approximately represents the ¹⁴C/C of atmospheric CO₂ in the year 1890.

[14] We used an elemental mass balance approach for calculating net loss or gain to the forest floor. This method

is designed to quantify net elemental changes to the soil profile where elements can be lost (i.e., during combustion), inherited (i.e., from dust or canopy ash), or conserved (stable relative to other elements [Brimhall *et al.*, 1992; White *et al.*, 1996]). We chose Fe, Al, and Si as stable indices for calculating elemental loss and gains during burning because these elements are not susceptible to combustion (discussed in more detail in section 4.3) yet are different in their behavior and abundance in the system. While Fe has been shown to be involved with pyrogenic reactions, it is not likely combusted during burning, its concentrations are not correlated with Al and Si, and it is abundant in both mineral and organic compounds. While Si can potentially be assimilated by plants, it is not combustible and is present in both organic and inorganic compounds. Al is also noncombustible but is more abundant in mineral than organic materials. Together, the combination of Fe, Al, and Si were used for the stable constituent S in the calculation of strain and tau [after Brimhall *et al.*, 1992],

$$\text{Tau } C_{(S)} = C_b / ((BD_u / BD_b) C_u) (\text{Strain}_b + 1) - 1, \quad (1)$$

where Tau is the net gain (+) or loss (−) of element, BD is bulk density, and S is a stable constituent such as Al or Ash assumed to be conserved during burning; the parentheses refer to the element used for S . The subscript u is unburned; the subscript b is burned; C is the combusted element. Strain is a measure of mass change and is equal to $((BD_u / S_b) (S_u / BD_b)) - 1$. This equation can be rearranged as

$$\text{Tau } C_{(S)} = [1 - ((C_b / C_u) / (S_b / S_u))] \times -1, \quad (2)$$

revised from White *et al.* [1996].

[15] Because char represents a condensed burned product, we needed to compare charred layers to the proper unburned soil layers from which it was derived. For this, we used a “composite” depth-weighted average of the unburned soil layers by multiplying the soil constituent (%C, bulk density, %N, etc.) by the thickness of each soil layer, summing the soil constituent across all relevant soil layers (successively, starting with LM + DM, then LM + DM + UD, etc.), and dividing by total thickness. This weighting scheme was applied to the two unburned profiles at UPBS on Helmer’s Ridge (see Table 4 in section 4.3). We argue that these composite data offer a better estimate of fuel composition, since a char layer found in a UD soil layer likely represents the burned products of LM, DM, and, potentially, UD layers.

4. Results

4.1. Physical Changes by Burning

[16] The unburned soil layers showed increases in bulk density and many chemical constituents with depth (Table 1). The most dramatic chemical changes occurred between the dead moss and upper duff soil layers. Carbon concentrations stayed relatively constant throughout the live moss, dead moss, and upper duff layers, but were significantly lower in the lower duff soils (Tables 1 and 2). However, using a backward selection, general linear model

(SAS/SYSTAT operating system, version 4.10, 1998, from SAS Institute, Cary, North Carolina), both depth (partial $R^2 = 0.1394$; $F = 3.63$; $p = 0.0531$) and bulk density ($R^2 = 0.4384$; $F = 9.37$; $p = 0.0099$) were significant predictors of C concentrations, together explaining about 60% of the variation in %C across our unburned samples. Data agree with the regression equation for %C and bulk density of Rapalee *et al.* [1998] for black spruce forest soils in Manitoba.

[17] Soil layers on the forest floor at Helmer’s Ridge averaged 14 cm in thickness (Table 1) before the burn and were reduced by an average of 9 cm (Table 2), resulting in a thickness of about 5 cm post-burn. Burned samples had slightly higher bulk densities (0.025 ± 0.007 , $n = 5$) than unburned samples (0.016 for LM to 0.024 for DM) but the differences were not statistically significant (Table 2). In general, the concentrations of most elements varied by burning (burned versus unburned layers) and with depth (LM, DM, UD, and LD layers) but did not vary by a burning-depth interaction (Table 1).

4.2. Changes in Elemental Abundance: Layering and Burning

[18] Concentrations of C, N, Ca, Mn, and P varied significantly among soil layers and with burning status, but did not vary according to a soil layer \times burning interaction (Tables 1 and 2). However, Mg varied only with burning, showing increased concentrations post-fire, and Si varied only with depth (Table 1). Unlike other elements, Al and Hg did not change significantly in concentration with either layering or burning. As noted above, C and N concentrations increased with burning and decreased with depth. For the uppermost soil layers, there was a 10 to 47% increase in C concentration and a 51 to 160% increase in N following burning. ^{13}C increased with depth by 4–5 per mil between the uppermost moss layers and the LD (Oa) layers (Tables 1 and 2).

[19] While the univariate analyses described above show trends in individual chemical constituents with depth or burning, canonical discriminant analysis was used to analyze 15 element concentrations simultaneously (Table 1). The first canonical axis was dominated by C and aluminosilicate elements and separates the soil layers, particularly the LD, from other layers (Figure 3). The second canonical axis, which is dominated by macronutrients, separates burned from unburned layers, particularly for LD layers. This analysis suggests that the chemistry of lower duff soil layers varies from other soil types, and highlights the importance of C, Al, and Si concentrations in separating soil chemistry with depth.

[20] Using correlation analysis to determine which chemical constituents behave similarly upon burning, we specifically tested for correlations across four groups of elements, including combustibles, major cations or nutrients, redox elements, and aluminosilicates (Table 3). C and N concentrations in our burned samples (r^2 values above the black boxes) were not significant (Pearson’s r^2 is -0.46 , but this is not significant). However, when C and N data were expressed as ratios of burned:unburned samples (for example, Cb/Cu regressed against Nb/Nu), significant and

Table 1. Elemental Chemistry for Unburned and Burned Soil Layers at the Frostfire Experimental Burn^a

Statistic	Bulk Density	Thickness	%C	¹³ C	N, %	Na ₂ O, %	K ₂ O, %	CaO, %	MgO, %	MnO, %	Fe ₂ O ₃ , %	Al ₂ O ₃ , %	SiO ₂ , %	P ₂ O ₅ , %	Hg, ppm
<i>Unburned Layers</i>															
Unburned LM layer	0.016	2	45.33	-30.17	0.56	0.04	0.32	0.38	0.11	0.08	0.13	0.17	1.00	0.17	0.068
average	0.010	1.00	0.68	0.61	0.12	0.03	0.01	0.04	0.01	0.00	0.02	0.00	0.24	0.00	0.016
st deviation	55	55	2	2	2	2	2	2	2	2	2	2	2	2	2
Unburned DM layer	0.024	4	45.61(a,2)	-29.03	0.55(a,2)	0.04(a)	0.16(a,2)	0.24(a,2)	0.08(2)	0.04(a,2)	0.16(a)	0.37	1.49(a)	0.11(a,2)	0.069
average	0.010	4	0.41	0.41	0.08	0.02	0.07	0.16	0.03	0.03	0.05	0.12	0.53	0.04	0.034
st deviation	91	91	5	5	5	5	5	5	5	5	5	5	5	5	5
Unburned UD layer	0.050	7	46.34(b,2)	-27.03	0.83(b,2)	0.33(ab)	0.55(b,2)	0.39(b,2)	0.31(2)	0.03(b,2)	0.76(b)	3.49	14.04(ab)	0.33(b,2)	0.135
average	0.068	5	5.15	0.63	0.13	0.26	0.34	0.19	0.20	0.02	0.33	2.71	11.40	0.13	0.038
st deviation	121	121	4	3	4	4	4	4	4	4	3	4	4	4	4
Unburned LD layer	0.172	1	16.92(b,2)	-25.74	0.60(b,2)	0.84(b)	1.63(b,2)	0.71(b,2)	0.90(2)	0.03(b,2)	3.57(b)	10.16	42.79(b)	0.33(b,2)	0.098
average	0.114	1	8.23	0.83	0.31	0.15	0.19	0.02	0.23	0.01	0.99	1.71	10.83	0.16	0.048
st deviation	16	16	3	3	3	3	3	3	3	3	3	3	3	3	3
<i>Burned Layers</i>															
Burned DM layer	0.025	3	56.93(a,1)	-28.8	1.17(a,1)	0.18(a)	0.76(a,1)	1.44(a,1)	0.37(1)	0.29(a,1)	0.60(a)	1.25	4.50(a)	0.53(a,1)	0.079
average	0.007	1	3.06	.85	0.18	0.13	0.35	0.72	0.21	0.14	0.64	1.24	3.92	0.25	0.02
st deviation	5	5	8	8	8	8	8	8	8	8	8	8	8	8	8
Burned UD layer	0.028	1	54.05(b,1)	-27.86	1.29(b,1)	0.32(ab)	1.21(b,1)	2.98(b,1)	0.58(1)	0.62(b,1)	1.11(b)	2.30	10.08(ab)	0.80(b,1)	0.079
average	0.022	0.50	8.00	.73	0.26	0.14	0.20	1.09	0.12	0.27	1.08	1.71	6.54	0.22	0.02
st deviation	5	5	5	5	5	5	5	5	5	5	5	5	5	5	5
Burned LD layer	0.159	1	31.42(b,1)	-26.51	1.49(b,1)	0.75(b)	1.47(b,1)	1.21(b,1)	0.84(1)	0.16(b,1)	3.55(b)	7.82	34.78(b)	0.58(b,1)	0.069
average	NA	1	NA	.71	NA	NA	NA	NA	NA	NA	NA	NA	NA	NA	NA
st deviation	1	1	1	2	1	1	1	1	1	1	1	1	1	1	1
count	1	1	1	1	1	1	1	1	1	1	1	1	1	1	1

^aFor each element or compound except ¹³C (which we did not include in the statistics), we used a two-way nonparametric ANOVA using data in Table 2. Means with same-letter or same-number superscripts do not vary from one another (p < 0.050). Where numbers and letters are used as superscripts, elements varied significantly by burning (1 df) and by layering (2 df) with no significant burning × layer interaction; letters refer to soil layers (DM, UD, and LD) while numbers refer to burning (unburned, burned). Where only letters are used as superscripts, elemental chemistry varied significantly by layering without a significant burning effect or burning × layer interaction. Unburned live moss layers (LM) were not included in the ANOVA to ensure balance of our model.

Table 2. Field and Laboratory Data for Individual Soil Layer Samples From Burned and Unburned Sites^a

Replicate	Code	Sample	Layer Burned Into	Thickness, cm	CM Reduction	Height Above Mineral	BD	C, %	N, %	¹³ C	LOI	Na ₂ O, %	K ₂ O, %	CaO, %	MgO, %	MnO, %	Fe ₂ O ₃ , %	Al ₂ O ₃ , %	SiO ₂ , %	P ₂ O ₅ , %	TiO ₂ , %	Ba, ppm	Sr, ppm	Hg, ppm
1	b	a1(6).2	DM	2	5	10	0.016	58.19	1.23	-29.40	92.74	0.157	0.709	1.423	0.320	0.200	0.266	0.633	2.904	0.509	0.038	157.542	0.000	0.070
2	b	a2(7).1	DM	1	MD	11	0.034	55.25	1.18	-28.09	88.21	0.125	0.967	1.240	0.348	0.302	0.933	1.188	5.037	0.604	0.231	174.907	43.000	0.074
4	b	FFS5A4(7).2	UD	2	11	15	0.027	58.97	1.72	-27.99	85.16	0.258	1.110	2.271	0.608	0.205	0.816	1.692	7.554	0.788	0.174	320.544	72.271	0.074
5	b	FFS5A5(7).8	LD/A	8	21	5	0.159	37.69	1.37	-26.01	35.84	0.975	2.162	1.508	1.123	0.257	5.178	10.522	48.056	0.597	1.027	821.248	149.493	0.114
6	b	FFS5A6(7).1	DM	1	10	10	0.032	56.55	0.92	-28.30	72.18	0.470	1.461	2.061	0.854	0.442	2.056	4.145	13.799	1.066	0.440	506.324	111.280	0.073
7	b	FFS5A7(7).2	DM	2	7	26	0.021	50.89	1.43	-27.57	96.92	0.051	0.289	0.801	0.128	0.202	0.104	0.268	1.232	0.216	0.014	75.152	24.794	0.074
8	b	FFS5A8(4).4	LD	4	16	22	0.059	25.15	1.61	-27.02	67.41	0.531	0.772	0.916	0.554	0.062	1.923	5.117	21.509	0.567	0.280	570.325	93.207	0.024
9	b	FFS5A11(7).2	DM	2	5	17	0.014	58.21	0.98	-29.71	92.33	0.130	0.775	1.081	0.413	0.250	0.249	0.640	2.646	0.428	0.035	137.293	24.621	0.054
10	b	FFS5A12(4).2	UD	2	7	15	0.016	58.78	1.32	-28.17	89.79	0.207	1.031	1.848	0.470	0.392	0.377	0.999	4.155	0.556	0.049	230.746	49.008	0.065
11	b	FFS5A13(6).3	UD	3	11	15	0.014	51.473	1.093	-27.69	80.94	0.305	1.208	2.897	0.522	0.398	0.740	1.874	9.435	0.720	0.109	430.756	114.360	0.110
12	b	FFS5A14(2).1	DM	1	5	17	0.024	61.09	1.06	-29.97	93.50	0.140	0.504	0.852	0.288	0.142	0.328	0.631	2.698	0.381	0.053	101.400	23.660	0.083
13	b	FFS5A15(7).3	UD	3	18	3	0.066	40.96	1.29	-26.73	63.41	0.560	1.537	4.684	0.765	1.061	3.011	5.306	21.259	1.164	0.706	731.800	177.827	0.081
14	b	FFS5A16(7).4	UD	4	8	10	0.016	60.17	1.07	-28.71	85.04	0.259	1.144	3.216	0.530	0.657	0.585	1.631	8.019	0.761	0.087	384.472	98.736	0.063
15	b	FFS5A17(13).1	DM	1	3	3	0.032	56.08	1.39	-28.42	90.60	0.165	0.527	1.100	0.257	0.250	0.457	1.598	3.957	0.457	0.055	398.560	73.038	0.111
16	b	FFS5A18(7).2	DM	2	2	9	0.017	59.15	1.17	-28.97	88.71	0.227	0.811	2.935	0.361	0.567	0.376	0.898	3.714	0.607	0.046	380.473	116.287	0.094
17	u	UPBS5.2	LM	2	NA	8	0.016	45.81	0.65	-30.60	97.32	0.017	0.316	0.410	0.102	0.078	0.112	0.228	0.829	0.170	0.012	45.106	13.035	0.056
18	u	UPBS5.5	DM	3	NA	5	0.024	45.33	0.67	-29.73	96.48	0.033	0.271	0.505	0.108	0.078	0.176	0.391	1.535	0.163	0.021	72.740	17.868	0.072
19	u	UPBS5.7	UD	2	NA	3	0.050	40.08	0.75	-26.62	81.49	0.263	0.499	0.336	0.263	0.020	1.000	2.946	11.367	0.302	0.156	294.970	42.265	0.131
20	u	UPBS5.10	LD	2	NA	0	0.172	20.29	0.85	-25.06	41.67	0.846	1.533	0.705	0.769	0.023	3.046	9.883	38.014	0.425	0.568	660.935	96.604	0.087
21	u	UPBS6.2	LM	2	NA	18	0.016	44.85	0.48	-29.74	97.23	0.061	0.327	0.357	0.119	0.082	0.140	0.319	1.172	0.169	0.016	38.780	9.279	0.079
22	u	UPBS6.5	DM	3	NA	5	0.024	45.48	0.51	-28.66	96.71	0.065	0.197	0.261	0.102	0.050	0.185	0.477	2.007	0.144	0.026	53.627	10.725	0.073
23	u	UPBS6.10	DM	5	NA	10	0.024	46.13	0.47	-28.90	98.01	0.030	0.098	0.135	0.047	0.026	0.081	0.188	0.724	0.077	0.010	23.880	5.174	0.099
24	u	UPBS6.15	DM	5	NA	5	0.024	45.18	0.51	-28.84	97.41	0.041	0.099	0.134	0.061	0.022	0.132	0.319	1.246	0.088	0.017	35.742	7.925	0.090
25	u	UPBS6.19	DM	4	NA	1	0.024	45.95	0.61	-29.00	96.96	0.055	0.135	0.144	0.072	0.006	0.206	0.480	1.961	0.095	0.027	51.984	12.707	0.013
26	u	UPBS6.20	UD	1	NA	0	0.050	44.40	0.96	-27.76	93.53	0.115	0.215	0.193	0.137	0.016	0.375	1.087	4.969	0.178	0.064	137.811	24.133	0.173
27	ua	FFS5A2(7).3	DM	2	NA	7	0.05	51.01	0.87	-27.29	91.87	0.116	0.446	0.438	0.207	0.072	0.454	1.154	4.722	0.293	0.068	142.851	27.246	0.117
28	ua	FFS5A2(7).6	UD	3	NA	4	0.10	51.67	0.92	-26.72	84.86	0.224	0.465	0.388	0.258	0.038	0.891	2.545	9.158	0.338	0.137	257.699	39.366	0.153
29	ua	FFS5A2(7).9	LD	3	NA	1	0.10	22.93	0.69	-26.66	47.63	0.689	1.503	0.698	0.765	0.034	2.958	8.608	35.161	0.414	0.563	560.368	92.264	0.151
30	ua	FFS5A2(7).10	LD	1	NA	0	0.40	7.53	0.25	-25.49	17.81	0.990	1.844	0.731	1.165	0.040	4.711	11.987	55.184	0.151	0.812	643.070	110.021	0.056
Composite	u	Average	LM, DM	8	NA	5	0.022	47.38	0.68	1.40	95.34	0.06	0.29	0.36	0.13	0.06	0.25	0.61	2.45	0.19	0.03	81.24	12.36	0.08
St deviation	-	-	-	3.0	NA	4.0	0.009	3.15	0.18	-1.39	3.02	0.05	0.15	0.16	0.07	0.03	0.18	0.47	1.97	0.10	0.03	54.53	5.05	0.03
count	-	-	-	27	NA	3	27	3	3	3	3	3	3	3	3	3	3	3	3	3	3	3	3	3
Composite	u	Average	LM, DM, UD	14	NA	2	0.028	46.95	0.71	1.15	92.65	0.10	0.32	0.34	0.15	0.05	0.41	1.10	4.21	0.21	0.06	124.24	16.51	0.10
St deviation	-	-	-	3.4	NA	2.1	0.005	3.88	0.18	-0.94	4.40	0.06	0.16	0.14	0.08	0.02	0.26	0.73	2.69	0.10	0.04	78.16	9.83	0.03
count	-	-	-	27	NA	3	27	3	3	3	3	3	3	3	3	3	3	3	3	3	3	3	3	3
Composite	u	Average	LM, DM, UD, LD	16	NA	0	0.057	37.65	0.75	0.80	73.15	0.36	0.81	0.52	0.41	0.05	1.48	4.30	17.27	0.30	0.26	320.35	45.40	0.11
St deviation	-	-	-	4.2	NA	0	0.016	1.11	0.02	0.36	5.74	0.06	0.14	0.01	0.11	0.00	0.40	0.83	4.19	0.04	0.07	45.58	0.01	0.03
count	-	-	-	2	NA	2	2	2	2	2	2	2	2	2	2	2	2	2	2	2	2	2	2	2

^aLayers defined as in Table 1. NA, not applicable; MD, missing data; b, burned sample including ash; u, unburned sample; ua, unburned sample beneath burned surface; BD, bulk density in g/cm³.

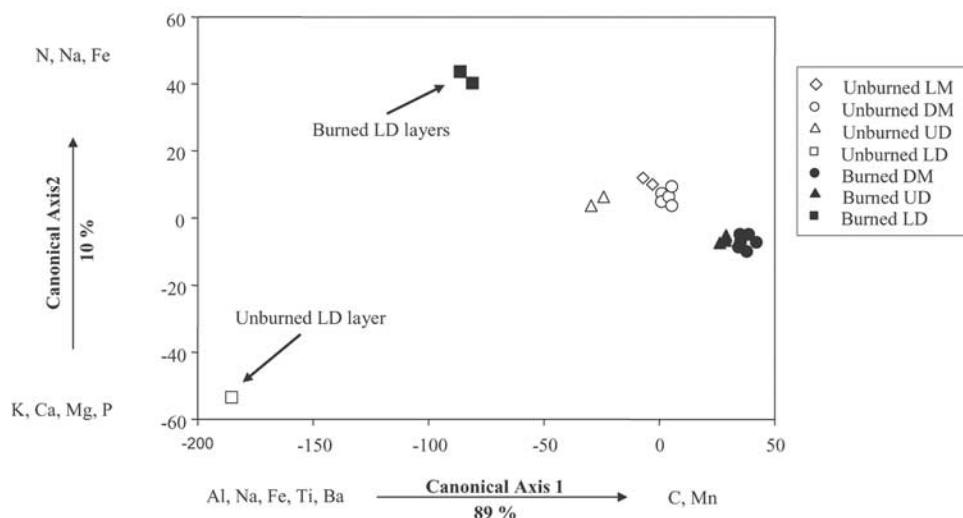


Figure 3. Canonical discriminant analysis of 15 chemical variables in burned and unburned soil layers at the FROSTFIRE Experimental Burn.

positive correlation (r^2 0.83) suggests that the change in the mass balance of these elements during fire are similar. Some cations and nutrients such as Na, K, Ca, Mg, and P were positively correlated to one another (Table 3), as were the aluminosilicates (Al and Si).

4.3. Burn Severity and Combustion

[21] The relationship between burn severity and post-burn chemical and physical properties is defined by both pre-burn soil layering and the chemical and physical effects of burning. We examined the relationship between burn severity (total reduction of soil layers in centimeters, measured via metal pin methods described above) and soil properties. Element redistribution by fire involves a decrease in the concentration of combustible elements such as C (Figure 4a), which is complicated by the fire penetrating

deeper and less C-rich layers, an increase in concentration of noncombustible elements (Figure 4b), and a slight increase in bulk density (Figure 4c), which is also affected by deeper layers. Therefore, as severity is increased, increases in bulk density and decreases in %C with depth have opposing effects on consequential C emissions.

[22] The use of Tau (equation (2)) helps to unravel confounding effects of density, concentration, and net loss of elements. Using Tau-based calculations and composite fuel variables, our estimates show an increase in combustion losses with increasing severity (Figure 4d). According to this approach, there was a loss of about 1000–2000 g organic matter and 600–1400 g C per m² from the UPBS site, an estimate that overlaps with direct inventories of unburned and burned samples (Table 4). Tau-derived estimates of combustion are based on composite fuels of only

Table 3. Pearson Correlation Coefficients for Four Groups of Element Concentrations in Soil, Including Combustibles, Major Cations, and Nutrients, Elements With Redox Potential, and Aluminosilicates^a

	Cm Reduction	Combustibles			Major Cations/Nutrients					Redox		Aluminosilicates	
		C, %	N, %	Hg, %	Na, %	K, %	Ca, %	Mg, %	P, %	Mn, %	Fe, %	Al, %	Si, %
C, %	-0.802	-	-0.46	0.23									
N, %	0.397	0.83	-	-0.14									
Hg, %	-0.009	-0.32	0.26	-									
Na, %	0.893				-	0.85	0.25	0.92	0.46				
K, %	0.779				0.65	-	0.48	0.95	0.67				
Ca, %	0.286				0.02	0.57	-	0.37	0.79				
Mg, %	0.863				0.87	0.94	0.38	-	0.66				
P, %	0.534				0.77	0.98	0.44	0.98	-				
Mn, %	0.237									-	0.16		
Fe, %	0.891									-0.45	-		
Al, %	0.888											-	0.99
Si, %	0.889											0.98	-

^aWithin each group, coefficients for element concentrations in burned soil samples are shown above the dashes. Coefficients for ratios of burned/unburned soil concentrations (e.g., Cb/Cu correlated with Nb/Nu) are shown below the dashes. Bold-faced text represents significant coefficients (p values corrected for multiple comparisons within each group of elements, n = 14 for burn coefficients and n = 4 for burn/unburn coefficients). Data are given in Table 2.

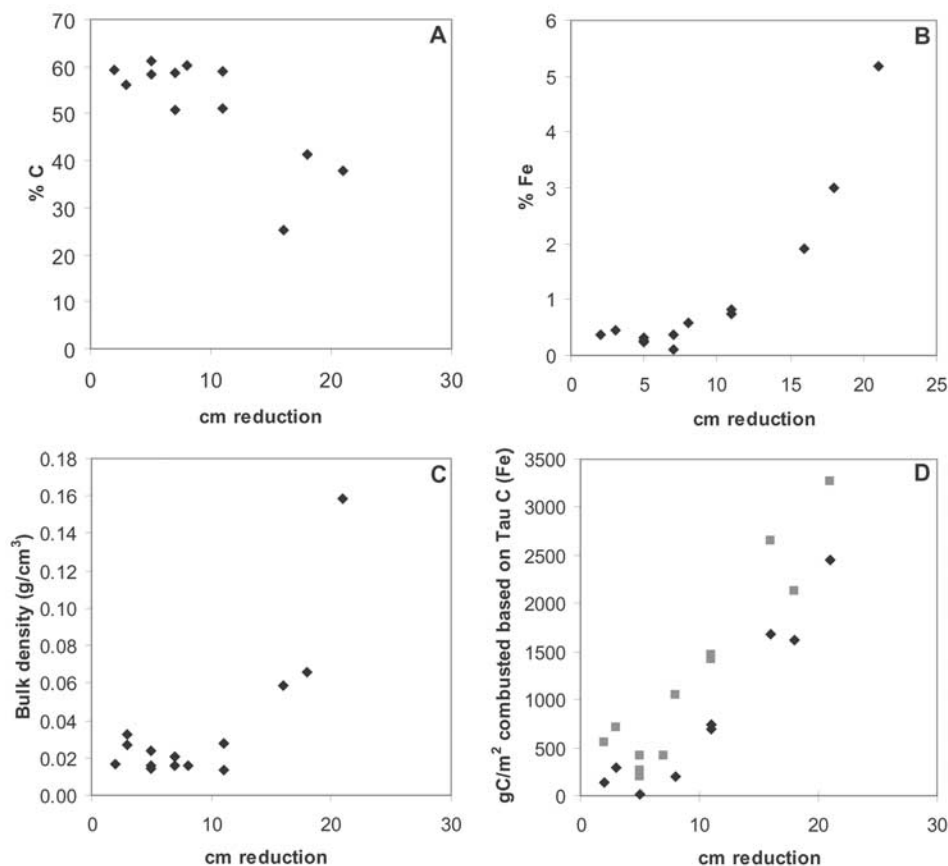


Figure 4. Individual ash/char samples plotted as a function of fire severity as estimated by pin reduction. (a) Changes in carbon concentrations, (b) Fe concentrations, (c) bulk density, and (d) combustion loss calculations based on composite fuels of the forest floor. Also shown in Figure 4d (circles) are calculations where composite fuels were adjusted to include needles and fine branches. Figure is based on data in Table 2 and equation (1).

the forest floor, yet the canopy clearly contributed to the ash as well. If ratios of the stable to combusted element in the canopy fuels differs from the ground fuels, then tau-derived estimates of combustion could be misleading. On the basis of a limited analyses of needles and fine branches, we recalculated tau-derived combustion rates to assess the importance of canopy ash. The revised Tau and composite fuel resulted in a slight increase in the estimate for C emissions (Figure 4d, open circles), largely because Fe_u concentrations and Fe_u/C_u ratios were significantly lower in canopy than forest-floor fuels. Our emissions therefore significantly underestimate the total emission (Table 4) from the site. In future work, a more complete analysis of fine fuels, bark, and coarse fuels should be included for Tau and inventories in order to assess the mass balance for the whole forest fire.

[23] Net gains relative to Fe, Al, and Si were indicated for most major nutrients within the forest floor (Figure 5). Gains, which reflect inheritance onto the forest floor from canopy ash and/or from ash blown in, were especially high for Ca and Mn. The inheritance of large amounts of Mn may be related to ash from spruce needles, which are high in Mn

(data not shown). Losses of C and Hg (Table 4) are quite similar according to Tau, despite the lack of correlation between Hg with other elements (Table 3). While solid phase combustion products of C result in increased C concentration by burning (Table 1), Hg appears to be more

Table 4. Combustion Losses of C, N, and Hg From the Forest Floor^a

	Fire Emission, g m ⁻²			
	OM	Carbon	Nitrogen	Mercury ($\times 10^{-4}$)
	<i>On the Basis of Tau (Fe, Al, Si)</i>			
Mean	1244	518	-4	2
Standard deviation	(1711)	(774)	(19)	(2)
	<i>Preburn-Postburn Inventories</i>			
Mean	2344	926	6	2
Standard deviation	(1211)	(860)	(31)	(3)

^aTau calculations are based on equation (1) in which average weight percent of Fe, Al, and Si are used as S in equation (1). Data for burned samples and unburned composite samples are shown in Table 2. Preburn minus postburn inventories calculated directly from average burned samples with chemistry, average bulk density, and thickness data in Table 3 and composite data in Table 2.

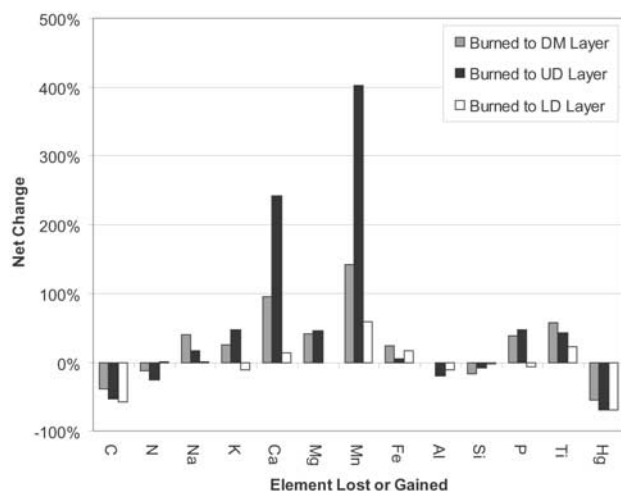


Figure 5. Net losses of elements resulting from burning of the forest floor, based on data in Table 2 and calculations of Tau using Fe, Al, and Si as S and using composite of unburned samples U (equation (1)). Tau values were averaged and plotted separately for burns into DM, UD, and LD layers using burned-layer averages in Table 1 and composite averages in Table 2. Standard deviations for these averages range from 6% net loss for C in LD burns to 36% net loss for Mn in DM burns.

completely combusted (Tau of 70%, Figure 5). As a result, the concentration of Hg in the burned ash + char sample reflects the concentration of the layer to which it burned, whereas %C reflects both the remaining layer and the charcoal that resides in the ash.

[24] While data in Figure 5 are tau-derived estimates of combustion using the averages of Si, Al, and Fe as the stable constituent, individual combustion estimates for Si, Al, and Fe alone vary anywhere from +25% (case of net Fe) to -17% (case of net Si). These ranges represent all of the uncertainties associated with ash inheritance, elemental variations in unburned fuel and ash, as well as measurement errors. Tau values within about $\pm 25\%$ of zero should not be considered as significantly different from zero. For example, net changes in N and, in some cases (LD burns), P, K, Ca, and Ti are less than 25%. Nutrients or combustible elements (C, Hg) are unacceptable choices as stable constituents as they are subject to significant change during burning. Concentrations of ash (estimated as 100% - loss on ignition at 550°C) was used by *Turetsky and Weider* [2001] and is a promising candidate for a stable constituent relative to organic matter as long as %C is determined separately, especially for soil layers. We have chosen to use Fe, Al, and Si for our stable constituent (equation (1)) but recognize the opportunity to further explore other elements that might separate forest floor from canopy ash as well as stoichiometric relationships of burning in general.

4.4. Structural Changes in Organic Matter

[25] Organic layers of unburned profiles indicate two major thermal-loss peaks that are derived from the moss and root material found near the soil surface (Figure 6a). In

one profile, these peaks persist for at least 4 decades as indicated by the enriched ^{14}C of the bulk organics. In another profile, the deep, older layer contains only small amounts of either of the major peaks seen in shallow layers, which is a sign of decomposition. Surface ash-char layers indicate two thermal loss peaks in most cases (Figures 6c and 6d), but the first thermally labile peak occurs at a higher temperature than unburned layers (Figures 6c and 6d). The second peak is somewhat enhanced in burned samples but also is obscured in severe fires, to almost merge with peak I (Figure 6d). The variability in peak area is greatest in the more severe fires that burned to the UD layers (Figure 6d).

5. Discussion

[26] Burning causes (1) large fluxes of combustible elements from terrestrial ecosystems to the atmosphere, (2) alteration of the physical state and arrangement of soils, and (3) changes in the chemical structure, nutrient content, and lability of residual organic matter. Changes in soil chemistry pre- and post-burn indicate short-term fluxes of combustible elements such as C, N, and Hg (Table 4; Figure 5), and presumably O, H, and S during combustion. The loss of these elements from soils is accompanied by the physical “collapse” of noncombustible elements onto a thinner forest floor. Nutrient cycling is affected by physical rearrangement of both organic and mineral phases. The deeper organic soil layers are also impacted, both physically, through changes in density and exposure, and chemically, through inheritance of nutrients from the canopy ash. Combined with transformations in structural chemistry and lability of the organic matter (“charring” effect), as well as albedo and active-layer thickening, these physical and chemical changes likely play a major role in boreal C and element cycling for several decades post-fire.

[27] There are basic differences in the way elements are vulnerable to combustion. Here we used several statistical approaches to examine variations in element abundance before and after fire activity, including univariate models, correlation analyses, and multivariate analysis. On the basis of heterogeneity in both fuels and combustion severity, N appears to have complex and variable responses to burning (Tables 3 and 4), perhaps in part because amino and aromatic structures can be combusted directly but can also form through coalification or distillation reactions during the wildfire. The close agreement of C and Hg combustion using Tau-calculations (Figure 5) suggests that Hg is combusted along with C and organic matter. While some Hg may enter the atmosphere in elemental form, some Hg remains in particular form in association with ash and char [*Friedli et al.*, 2001]. However, soil Hg concentrations are not affected by burning (Tables 1 and 3), suggesting that Hg lacks the charring effects seen for C (Table 1). Thus, while changes in weather and climate have been shown to influence combustion, we add that various chemical and structural properties of soils can respond variably to fire activity on a relatively small scale.

[28] Because of large spatial heterogeneity and the difficulty of sampling close in time to a burn, the methods presented here (use of Tau calculations) allow a sampling

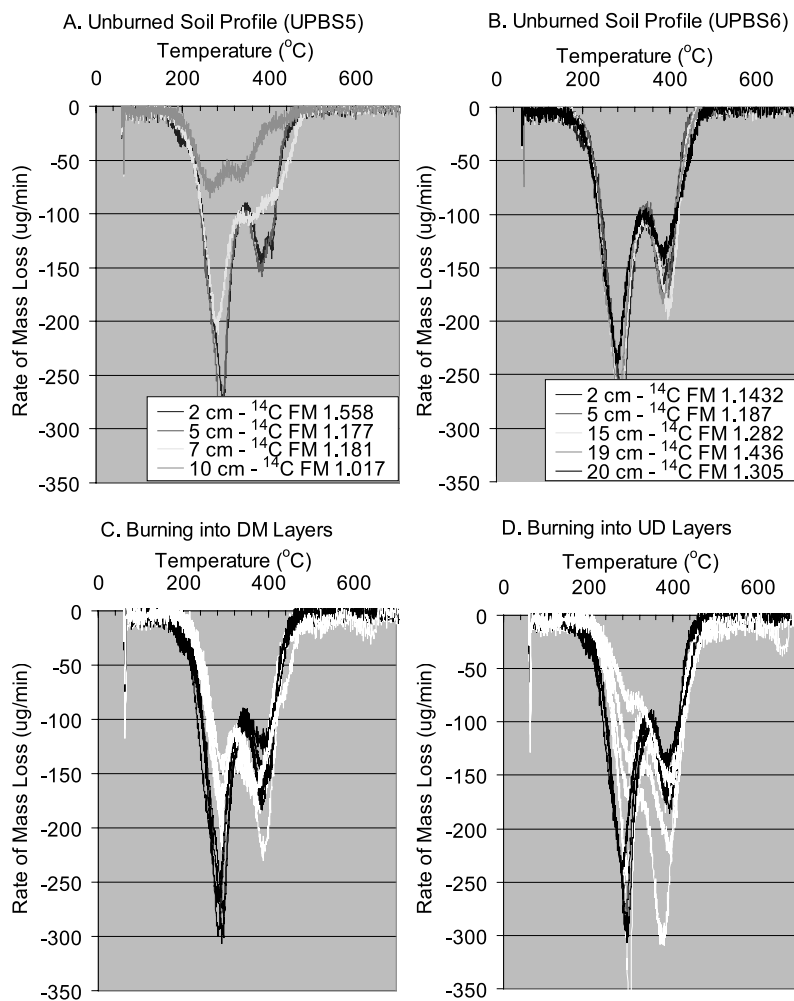


Figure 6. Rates of thermogravimetric loss of (a, b) unburned profiles showing radiocarbon contents (insert) and (c) burned surface DM and (d) burned surface UD layers containing ash. See color version of this figure at back of this issue.

regime that forgoes the measure of bulk density and thickness of the ash/charred layer by relying on bulk densities and thickness data of the unburned profiles combined with chemical compositions of both burned surface samples and unburned profiles. Relating element concentrations to net losses, gains, and retention (equations (1) and (2)) in this way is potentially very useful in situations where numerous replications are needed but time is limited, for example, immediately after a fire when access is brief or requires escort by professional fire staff. The use of Tau still requires, however, a careful assessment of an unburned control site in which layers are recognizable in both pre- and post-burn materials. Moreover, the variations in combustion losses are great and indicate a need for large sample sizes and layer-stratified samples.

5.1. Nutrients and Burning

[29] The shifts in nutrient pools, evident from pre- and post-burn inventories (Table 4), have implications for recovering vegetation and C cycling. The shift in C/N ratios from about 60 in unburned to 40 in burned layers (Table 1)

indicates a greater combustion loss of C than N (Figure 4) [see also *Harden et al.*, 2003], but site-to-site variability in forest floor chemistry is large. While *Harden et al.* [2003] suggest that between 30 and 40% of forest-floor N was lost during average fire events in northern Manitoba, the N losses measured here are not significantly different from zero and were highly variable among plots. Below the ash and char layers at the FROSTFIRE sites, about 20 to 40 gN/m² remain as unburned organic material, which depending on chemical form and bioavailability, may be available as a fire fertilization effect. One of the central controls over long-term C fluxes in boreal systems is the short-term change in N availability after a fire and the long-term implications of volatile N loss due to burning [*Harden et al.*, 2003]. The changing C:N ratios observed in this study suggest the potential for increasing N turnover and availability post-fire, which is consistent with elevated levels of total N that we have found in soil lysimeters after a wildfire near Delta Junction (J. Neff, unpublished data, 2003). In addition to changes in nutrient content, changes are also likely in microbial composition [see, e.g., *Acea and*

Carballas, 1996], and other physical effects, such as both temperature and available moisture in surface soils, may impact nutrient cycling and availability post-fire [*Viereck et al.*, 1983; *O'Neill et al.*, 2003].

[30] Across all soil layers, concentrations of P increased significantly with burning (Table 1). Phosphorus concentrations ranged from 0.7 to 10 g P/m² after the burn. Black spruce systems utilize P at rates ranging from 0.02 to 0.12 g P/m²/yr [*Van Cleve et al.*, 1983], suggesting that fire-induced P fertilization can last anywhere from 5 to 500 years for regrowing spruce. With greater nutrient demands, aspen would require 5 to 10 times as much P as spruce recovers, though this is expected to decline once a P stock of about 3 g P/m² is stored in the mature aspen stand [*Van Cleve et al.*, 1983]. While these numbers suggest that P utilization by plants is variable, we show here that the spatial heterogeneity in ash and its P content also are variable.

5.2. Organic Matter Transformations

[31] Transformations of carbon compounds are evident from combustion estimates and thermogravimetry. *Schuur et al.* [2003] used the isotopic composition of CO₂ during the FROSTFIRE experiment to estimate combustion losses of 2.5 kg C/m². Similarly, the LOI-based combustion calculation of *Turetsky and Weider* [2001], as applied to the data of this experiment, resulted in an estimate of 3000 ± 6200 g organic matter, which is 50% greater than the estimates based on Tau. Unburned live moss and dead moss layers contain about 45% C with about 97% LOI, whereas burned DM layers contain about 55% C with about 90% LOI (Tables 1 and 2). Thus fire alters the relationship between C and organic matter with depth in soil layers, and thermally stable C in ash might account for differences between some combustion estimates.

[32] Thermogravimetry lends some insights into the LOI-C shifts seen in burned samples. There is a shift of the first “thermolabile” mass-loss peak toward higher temperatures when unburned samples are compared to burned samples (Figure 6), and there is a shift at higher temperatures as well. On average, about 1.7 (±0.91) mg of C were lost at temperatures between 550 and 1000°C for burned samples, whereas only 0.7 (±0.16) mg C were lost from the unburned layers at these high temperatures. Analyses of coal, which is derived from organic matter and fire ash, conventionally report mass-loss yields for both labile “S1” and chain or lignin-like “S2” forms [*Marshall et al.*, 2002]. Using strict (“Rock-Eval” pyrolysis) definitions for S1 (mass lost between 150° and 300°C) and S2 (mass lost between 300° and 500°C), we found the following mass loss percentages: unburned LM, DM, UD layers had 39 ± 8 percent S1 and 44 ± 6 percent S2, whereas burned DM and UD layers (with ash) had 24 ± 9 percent S1 and 51 ± 13 percent S2.

[33] Thermolabile forms of Hg have been shown for temperatures <30°C, a form which is climatically sensitive [*Martinez-Cortizas et al.*, 1999] and for much higher temperatures of 200° to 300°C, which typically indicates humus-bound or chloride-bonded Hg [*Beister and Zimmer*, 1998]. Our TG data (Figure 6) are consistent with the

combustion loss of organic-bound forms of Hg. While burning of organic layers is not analogous to the genesis of coal, the effects of burning do indicate a reduction of the S1 thermolabile pool and a slight increase in lignin-like [*Marshall et al.*, 2002] structures. In the long term, the creation of biologically recalcitrant C pools during fires could play an important role in the decadal to millennial stabilization of carbon in these ecosystems.

[34] This “charring effect,” while incomplete and heterogeneous, necessitates a careful accounting and definition of organic carbon in unburned and burned samples in order to accurately estimate combustion losses. Fire-induced generation of biologically labile and recalcitrant forms is unclear [see, e.g., *Viereck et al.*, 1983; *Acea and Carballas*, 1996; *O'Neill et al.*, 2003; *Schuur et al.*, 2003] as is correlation, if any, between thermolabile and biologically labile forms of carbon. Implications for microbial responses to the structural transformations of organic compounds and to the element distributions are also unexplored, for example, enzyme activity requiring trace metals such as Ni may be enhanced by burning because of the enrichment of non-combustible nutrients onto the forest floor. Overall, higher C concentrations in charred material compared to unburned soils (Table 1) suggest that burning is a mechanism of C loss (Table 4). Changes in the relationship between C and organic matter concentrations, however, suggest that fires also help to contribute charcoal to the system; while some of this char may be short lived [*Czimeczik et al.*, 2003], other more stable forms may contribute to long-term terrestrial net ecosystem production.

5.3. Impacts of Combustion on Atmosphere and Terrestrial Systems

[35] Wildfire is a key agent of environmental change through its sensitivity to climate and its impact on the physical and thermal state of the soil, nutrient stocks, and nutrient availability. Physical and thermal impacts of fire are particularly profound in boreal forests because of the sensitivity of near-surface permafrost in these regions [*Yoshikawa et al.*, 2002; *Viereck et al.*, 1983; *O'Neill et al.*, 2003]. The impacts of wildfire on boreal nutrients are also important because losses of N can limit the regrowth of forests after fire.

[36] Boreal wildfires may be a particularly large atmospheric source of Hg [*Friedli et al.*, 2003]. Generally, boreal forests are prone to severe fires that consume much of the forest floor and that are particularly widespread [*Kasischke and Stocks*, 2000]. Deeper organic layers found in wetter and colder environments have even greater stores of Hg than were reported for the UPBS sites in this report. For example, a poorly drained site at the base of the watershed had concentrations up to 360 ppm Hg in a lower duff Oa horizon at 35 to 29 cm depth (data not shown); with a bulk density of 0.25 g/cm³, this layer alone could contribute 12 * 10⁻⁴ g/m² of Hg in the event of a severe fire. Like C, which in deep layers of many peats and wetlands is protected from fire in all but the driest periods [*Tolonen*, 1985; *Kuhry*, 1994; *Harden et al.*, 2000; *Carcaillet et al.*, 2001], Hg in deep layers of wetland or permafrost soils may reflect protection from fire by saturated conditions. In boreal

forests, the areal extent of fires has varied tenfold as a result of summer drought cycles [Kasischke and Stocks, 2000]. Therefore Hg emissions from these regions are potentially very large and extremely variable on decadal to century timescales when eventually the right conditions for severe fires are likely to occur. As methylated forms of Hg are found in lowland, wetland, and lacustrine settings and are a health hazard in these forms [Mahaffey, 1999], severe fires could potentially remove Hg from lowland sources and redistribute it in both ash and gaseous forms. Since most managed fires, however, are prescribed for wetter weather not conducive to wetland burns, the most significant redistribution is likely to originate from wildfires during extreme droughts of the fire season.

[37] Whether prescribed or mitigated, fires and fire management policies have significant effects on atmospheric and terrestrial systems. Boreal wildfires could be a particularly large atmospheric source of not only C and N but also Hg, as boreal forests are prone to severe fires that consume much of the forest floor. Implications for N redistribution by fire are great because most forests and rangelands include some type of fire policy and because many systems are N limited. Heterogeneity of both fuel types and fire behavior may further complicate our understanding of C, N, and Hg losses to fire. Therefore more data for landscape/fuel type/fire behavior combinations are needed for newly burned, mature, and recovering ecosystems before we can develop predictive models and policies for estimating and managing C, N, or Hg stocks using fire.

[38] **Acknowledgments.** The competent organizers, fire fighters, fire escorts, and multitude of cooperative professionals made this seemingly small yet otherwise impossible study a reality. In addition, we are indebted to Terry Chapin and A. Dave McGuire for inviting and hosting our late participation in the experiment, to Elliott Spiker for supporting their invitation, to USFS personnel for welcoming and facilitating our involvement, and to R. Bolton, L. Hinzman, and D. Valentine for logistical support. Bill Cannon inspired the analysis of Hg in these samples. We thank Jim Crock for analytical testing of Hg methods and E. Kasischke for review of an earlier draft. Funding for this work was provided by NSF-LTER program and USGS Earth Surface Dynamics Program.

References

- Acea, M. J., and T. Carballas (1996), Changes in physiological groups of microorganisms in soil following wildfire, *FEMS Microbiol. Ecol.*, *20*, 33–39.
- Beister, H., and H. Zimmer (1998), Solubility and changes of mercury binding forms in contaminated soils after immobilization treatment, *Environ. Sci. Technol.*, *31*, 2755–2763.
- Brimhall, G. H., O. A. Chadwick, C. J. Lewis, W. Compston, I. S. Williams, K. J. Danti, W. E. Dietrich, M. E. Power, D. Hendricks, and J. Bratt (1992), Deformational mass transport and invasive processes in soil evolution, *Science*, *255*(5045), 695–702.
- Canadian Agricultural Services Coordinating Committee (1998), *The Canadian System of Soil Classification*, 3rd ed., 187 pp., NRC Can. Res., Ottawa.
- Carcaillet, C., Y. Bergeron, P. H. Richard, B. Frechette, S. Gauthier, and Y. T. Prairie (2001), Change of fire frequency in the eastern Canadian boreal forests during the Holocene: Does vegetation composition or climate trigger the fire regime?, *J. Ecol.*, *89*, 930–946.
- Conard, S. G., and G. A. Ivanova (1998), Wildfire in Russian boreal forests: Potential impacts of fire regime characteristics on emissions and global carbon balance estimates, *Environ. Pollut.*, *98*, 305–313.
- Crock, J. G. F. E. Lichte, and P. H. Briggs (1983), Determination of elements in National Bureau of Standards' geological reference materials SRM 278 obsidian and SRM 688 basalt by inductively coupled argon plasma-atomic emission spectrometry, *Geostand. Newsl.*, *7*(2), 335–340.
- Czimeczik, C. I., C. M. Preston, M. W. I. Schmidt, and E.-D. Schulze (2003), How surface fire in Siberian Scots pine forests affects soil organic carbon in the forest floor: Stocks, molecular structure, and conversion to black carbon (charcoal), *Global Biogeochem. Cycles*, *17*(1), 1020, doi:10.1029/2002GB001956.
- Driscoll, K. G., J. M. Arocena, and H. B. Massicotte (1999), Post-fire nitrogen content and vegetation composition in sub-boreal spruce forests of British Columbia's central interior, *Can. For. Ecol. Manage.*, *121*, 227–237.
- Dyreness, C. T., and R. A. Norum (1983), The effects of experimental fires on black spruce forest floors in interior Alaska, *Can. J. For. Res.*, *13*, 879–893.
- French, N. H. F., E. S. Kasischke, B. S. Lee, B. J. Stocks, and J. P. Mudd (2000), Carbon released during fires in North American boreal forests during the 1980's, in *Fire, Climate Change and Carbon Cycling in North American Boreal Forests*, *Ecol. Stud. Ser.*, edited by E. S. Kasischke and B. J. Stocks, pp. 377–388, Springer-Verlag, New York.
- Friedli, H. R., L. F. Radke, and J. Y. Lu (2001), Mercury in smoke from biomass fires, *Geophys. Res. Lett.*, *28*(17), 3223–3226.
- Friedli, H. R., L. F. Radke, R. Prescott, P. V. Hobbs, and P. Inha (2003), Mercury emissions from the August 2001 wildfires in Washington State and an agricultural waste fire in Oregon and atmospheric mercury budget estimates, *Global Biogeochem. Cycles*, *17*(2), 1039, doi:10.1029/2002GB001972.
- Gleixner, G., N. Poirier, R. Bol, and G. Balesdent (2002), Molecular dynamics of organic matter in a cultivated soil, *Org. Geochem.*, *33*, 357–366.
- Harden, J. W., S. E. Trumbore, B. J. Stocks, A. Hirsch, S. T. Gower, K. P. O'Neill, and E. S. Kasischke (2000), The role of fire in the boreal carbon budget, *Global Change Biol.*, *6*, suppl.1, 174–184.
- Harden, J. W., M. Mack, H. Veldhuis, and S. T. Gower (2003), Fire dynamics and implications for nitrogen cycling in boreal forests, *J. Geophys. Res.*, *108*(D3), 8223, doi:10.1029/2001JD000494.
- Hinzman, L. D., M. Fukuda, D. V. Sandberg, F. S. Chapin III, and D. Dash (2003), FROSTFIRE: An experimental approach to predicting the climate feedbacks from the changing boreal fire regime, *J. Geophys. Res.*, *108*(1), 8153, doi:10.1029/2001JD000415.
- Kasischke, E. S., and B. J. Stocks (2000), *Fire, Climate Change, and Carbon Cycling in the Boreal Forest*, 461 pp., Springer-Verlag, New York.
- Kuhry, P. (1994), The role of fire in the development of *Sphagnum*-dominated peatlands in western boreal Canada, *J. Ecol.*, *82*, 899–910.
- Liu, X., P. Van Espen, F. Adams, J. Cafmeyer, and W. Maenhout (2000), Biomass burning in southern Africa: Individual particle characterization of atmospheric aerosols and savanna fire samples, *J. Atmos. Chem.*, *36*, 135.
- Luc, L., and S. Luc (1998), Vegetation changes caused by recent fires in the northern boreal forest of eastern Canada, *J. Veg. Sci.*, *9*, 483–492.
- Mahaffey, K. R. (1999), Methyl mercury: A new look at the risks, *Publ. Health Rep.*, *114*, 397–402.
- Manies, K. L., J. W. Harden, S. R. Silva, P. H. Briggs, and B. M. Schmid (2002), Fate of carbon in Alaskan Landscapes Project: Soil data from a chronosequence near Delta Junction, AK, *U.S. Geol. Surv. Open File Rep.*, 02-62.
- Marshall, C. P., G. S. Kamali Kannangara, M. A. Wilson, J.-P. Guerbois, B. Hartung-Kagi, and G. Hart (2002), Potential of thermogravimetric analysis coupled with mass spectrometry for the evaluation of kerogen in source rocks, *Chem. Geol.*, *184*, 185–194.
- Martinez-Cortizas, A., X. Pontevedra-Pombal, E. Garcia-Rdeja, J. C. Novoa-Munoz, and W. Shotyk (1999), Mercury in a Spanish peat bog: Archive of climate change and atmospheric metal deposition, *Science*, *284*, 939–942.
- O'Neill, K. P., E. S. Kasischke, and D. D. Richter (2003), Seasonal and decadal patterns of soil carbon uptake and emission along an age-sequence of burned black spruce stands in interior Alaska, *J. Geophys. Res.*, *108*(D1), 8155, doi:10.1029/2001JD000443.
- Rapalee, G., S. E. Trumbore, E. A. Davidson, J. W. Harden, and H. Veldhuis (1998), Soil Carbon stocks and their rates of accumulation and loss in a boreal forest landscape, *Global Biogeochem. Cycles*, *12*, 687–701.
- Schimel, J., and A. Granstrom (1989), Fire severity and vegetation response in the boreal Swedish forest, *Ecology*, *77*, 1436–1450.
- Schuur, E. A. G., S. E. Trumbore, M. M. Mack, and J. W. Harden (2003), Isotopic composition of carbon dioxide from a boreal forest fire: Inferring carbon loss from measurements and modeling, *Global Biogeochem. Cycles*, *17*(1), 1001, doi:10.1029/2001GB001840.
- Soil Survey Staff (1998), *Keys to Soil Taxonomy*, 8th ed, 326 pp., U.S. Dep. of Agric., Washington, D. C.
- Stuiver, M., and H. Polach (1977), Reporting of ¹⁴C data, *Radiocarbon*, *19*, 355–363.

- Tolonen, M. (1985), Palaeoecological record of local fire history from a peat deposit in SW Finland, *Ann. Bot. Fenn.*, 22, 15–29.
- Trabaud, L. (1994), The effect of fire on nutrient losses and cycling in a *Quercus coccifera* garrigue (southern France), *Oecologia*, 99, 379.
- Turetsky, M. R., and R. K. Weider (2001), A direct approach and quantification of organic matter loss as a result of peatland wildfire, *Can. J. For. Res.*, 31, 363–366.
- Van Cleve, K. (1973), Short-term growth response to fertilization in young quaking aspen, *J. For.*, 71, 758–759.
- Van Cleve, K., and L. K. Oliver (1982), Growth response of postfire quaking aspen to N, P and K fertilization, *Can. J. For. Res.*, 12, 160–165.
- Van Cleve, K., L. Oliver, R. Schlentner, L. A. Viereck, and C. T. Dyrness (1983), Productivity and nutrient cycling in taiga forest ecosystems, *Can. J. For. Res.*, 13, 747–766.
- Van Wyk, D. B., W. Lesch, and W. D. Stock (1992), Fire and catchment chemical budgets, *Ecol. Stud. Anal. Synth.*, 93, 240–257.
- Viereck, L. A., C. T. Dyrness, K. Van Cleve, and M. J. Foote (1983), Vegetation, soils, and forest productivity in selected forest types in interior Alaska, *Can. J. For. Res.*, 13, 703–720.
- Vogel, J. S. (1992), A rapid method for preparation of biomedical targets for AMS, *Radiocarbon*, 34, 344–350.
- Wan, S., S. Hui, and Y. Luo (2001), Fire effects on ecosystem nitrogen dynamics: A meta-analysis, *Ecol. Appl.*, 11(5), 1349–1365.
- White, A. F., A. E. Blum, M. S. Schulz, T. D. Bullen, J. W. Harden, and M. L. Peterson (1996), Chemical weathering rates of a soil chronosequence on granitic alluvium: I. Quantification of mineralogical and surface area changes and calculation of primary silicate reaction rates, *Geochim. Cosmochim. Acta*, 60, 2533–2550.
- Yoshikawa, K., W. R. Bolton, V. E. Romanovsky, M. Fukuda, and L. D. Hinzman (2002), Impacts of wildfire on the permafrost in the boreal forests of interior Alaska, *J. Geophys. Res.*, 107(D1), 8148, doi:10.1029/2001JD000438.
-
- T. L. Fries, J. W. Harden, K. L. Manies, and M. R. Turetsky, U.S. Geological Survey, 345 Middlefield Road, MS 962, Menlo Park, CA 94025, USA. (tfries@usgs.gov; jharden@usgs.gov; kmanies@usgs.gov; mturetsky@usgs.gov)
- G. Gleixner, Max Planck Institute for Biogeochemistry, 07701 Jena, P.O. Box 100164, Germany. (gerd.gleixner@bgc-jena.mpg.de)
- J. C. Neff, Geological Sciences and Environmental Studies, University of Colorado, Boulder, CO 80309, USA. (neffjc@colorado.edu)
- R. Ottmar, Seattle Forestry Science Laboratory, 4043 Roosevelt Way NE, Seattle, WA 98105, USA. (ottmar@dorothy.cfr.washington.edu)
- D. V. Sandberg, Pacific Northwest Research Station, USDA Forest Service, 3200 SW Jefferson Way, Corvallis, OR 97331, USA. (dsandberg@fs.fed.us)

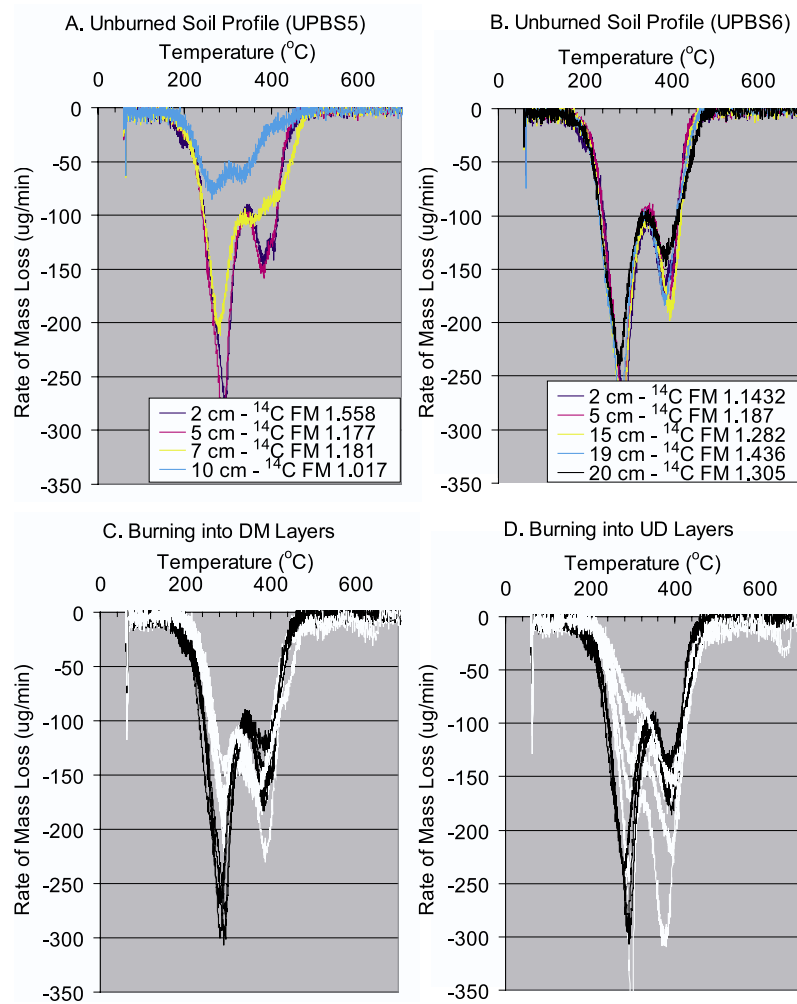


Figure 6. Rates of thermogravimetric loss of (a, b) unburned profiles showing radiocarbon contents (insert) and (c) burned surface DM and (d) burned surface UD layers containing ash.